

# DISSIMILAR METAL JOINTS FOR THE APT SUPERCONDUCTING CAVITY'S CRYOGENIC PLUMBING SYSTEM

M.J. Cola, M.B. Lyons, D.F. Teter and R.C. Gentzlinger\*

Materials Science & Technology—Metallurgy

\*Engineering Science and Applications—Design Engineering

Los Alamos National Laboratory, Los Alamos New Mexico, 87545

## Abstract

Titanium (Ti) is the material of choice for the helium (He) vessel surrounding the accelerator for the accelerator production of tritium (APT) superconducting cavities. The Ti helium vessel must be joined to a stainless steel (SS) cryogenic plumbing system in the cryomodule. In addition, a niobium (Nb) to SS joint must be developed that can replace a braze connection currently used to attach the stainless-steel Conflat flange to the Nb beam tube of the cavity. Inertia friction welding (IFRW) was chosen to ensure that sound joints were formed for both applications. IFRW is typically well suited for joining dissimilar metals. However, even this process has its limitations, particularly when the base metals are not physically or metallurgically compatible. Such incompatibilities can lead to the formation of brittle intermetallics at the interface; consequently, mechanical properties suffer. To remedy this, interlayer materials are used that are both structurally and microstructurally compatible with both base metals. The interlayer metal, while ideally at least as strong as the weakest base metal, is kept thin so that constraint effects will raise its apparent yield strength to match that of the base-metal yield strength. With this in mind, the main objective for the current study was to develop tube-to-tube parameters for joining 316L SS to Nb, and to commercially pure Ti using a Nb interlayer.

In the present study, welding parameters were developed and this paper highlights the salient microstructural features associated with the interface regions between the base metals and the interlayer metal, and reports on the mechanical properties of various joint combinations. To accomplish this, specimens were metallurgically prepared from as-welded and tested joints, and analyzed using light, scanning electron and transmission electron microscopy.

## 1. INTRODUCTION

Dissimilar metal joining Ti to other metals has met with limited success; brittle weldments result [1-7]. In response to this problem, an interlayer material was used by several researchers as a means of achieving sound, high-integrity joints between dissimilar metals [6,7]. Sassani and Neelam evaluated the feasibility of interlayer metals for joining incompatible base metals; less than optimal joint strengths were achieved [6].

A similar approach was attempted by Kou during friction welding trials using Alloy 718, Ti 6Al-2Sn-4Zr-2Mo and Ti 6Al-4V base metals [7]. Kou extended the concept of an interlayer to include two interlayer metals compatible with each other and their respective base metals. Results indicated an average as-welded joint strength of approximately 345 MPa, and PWHT strengths as high as 497 MPa. Finally, Kuo reports that a consistent relationship between weld strength and failure location remained elusive.

The present study investigated the metallurgical characteristics and mechanical properties of Nb to SS IFR welds, and Ti to SS IFR welds made with a Nb interlayer.

## 2. EXPERIMENTAL APPROACH

### 2.1 Material Preparation

The commercially available Ti and SS used in this study were in the form of 2-mm wall by 25-mm diameter tubes. A 25-mm diameter bar of Nb was the interlayer material. Prior to IFR welding, the tubes were sectioned into 75-mm lengths and the faying surfaces machined while bathed in alcohol. Additionally, the machining of the Nb bar provided a tubular geometry for joining to the SS and subsequently to the Ti. The Nb wall thickness was thicker (3.2-mm) than the tube's walls (2 mm) to provide for greater forging action during the welding cycle.

### 2.2 Friction Welding

IFR welds were produced using an MTI Model 90B inertia friction welding system. Two separate welds were made to achieve the final three-metal joint. First, SS was joined to Nb followed by a Nb to Ti weld. Separate parameters were developed for each weld joint. Since previous researchers work with Ti and SS did not employ an interlayer material, starting parameters were chosen because they were thought to be close to the optimum. Emphasis for this phase was on achieving weld joints capable of bending through 90 degrees. Once suitable starting parameters were developed, welds were made at various levels of rotational speed (60 to 188 m/min) and axial force (89 to 268 MPa) while maintaining a constant moment of inertia ( $0.16 \text{ kg}\cdot\text{m}^2$ ). After welding and prior to testing, each weld joint was He leak checked achieving a minimum leak rate of  $1 \times 10^{-10} \text{ atm}\cdot\text{cc/s}$ .

### 2.3 Weld Characterization

Visual examination was performed for weld axial displacement and flash. Disks about 3 mm in diameter were sectioned transverse, from the interlayer region of the Ti/Nb/SS welds. Thin foils were examined in a Philips CM30 analytical-electron microscope operated at 300 kV. Line scans across the Nb/SS interface region were performed using a VG HB601 scanning transmission electron microscope (STEM) operated at 100 kV and equipped with a Link ISIS EDS system.

Knoop microhardness testing (200-g load) was performed across the weld region at the axial centerline. Machining of full-scale tensile specimens removed weld flash and obtained a reduced-diameter of 24-mm over a gage length of 75-mm. In accordance with ASTM E8, testing was at an extension rate of 0.635 mm/min, and performed at 294 K and 77 K. Following mechanical testing, selected fracture surfaces were characterized using scanning electron microscopy.

## 3. RESULTS AND DISCUSSION

### 3.1 Macro and Microscopic Analysis

An as-welded Ti/Nb/SS IFR weld is shown in Figure 1. Consistent with the appreciably lower elevated-temperature strength of Ti relative to the Nb, these welds exhibited preferential flash formation in the Ti. A macrograph of an axially sectioned Nb/SS weld specimen is shown in Figure 2. Flash formation was predominately in the Nb. As expected, the axial displacement increased with an increase in axial force from 1 mm to 6 mm.

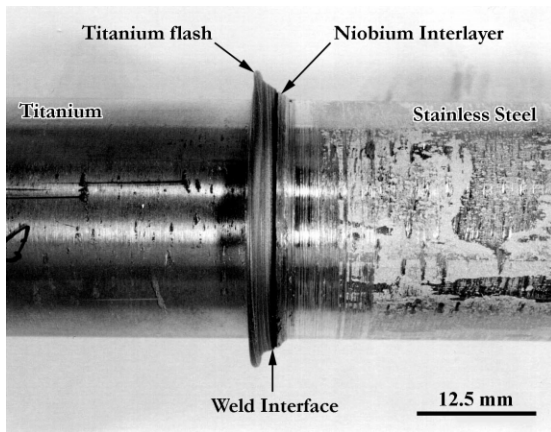


Figure 1. Photograph of as-welded Ti/Nb/SS joint.

### 3.2 TEM and STEM Analysis

A TEM micrograph of the as-welded 316L SS/Nb interface reveals a continuous interaction layer (Figure 3). Convergent beam electron diffraction patterns show that the interaction layer has a structure based on the NbFe<sub>2</sub> Cl<sub>4</sub> Laves phase. STEM line scans for Cr, Fe and Nb indicate a uniform distribution of these elements across the interaction layer (Figure 4). The sharp 316L

SS/NbFe<sub>2</sub> interface indicates Fe and Cr diffusion into the Nb, while the diffuse NbFe<sub>2</sub>/Nb interface suggests there was no Nb diffusion into the 316L SS.

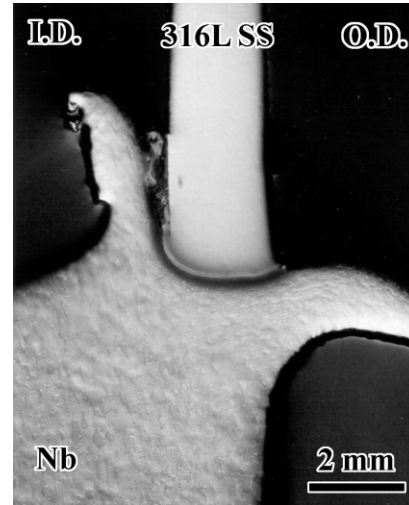


Figure 2. Macrograph of Nb/SS IFR weld. Notice the preferential flash formation in the Nb.

### 3.3 Hardness Testing

Knoop hardness traverses for each joint combination are shown in Figure 5. For the 316L SS/Nb weld, a slight hardness increase was observed near the weld interface in both metals. The increased hardness was attributed to cold worked metal near the interface resulting from deformation during the IFR weld process. KHN hardness measurements across the interlayer region of the Ti/Nb/SS weld also exhibited increased hardness near the interface because the cold worked metal was not extruded during the weld cycle. Additionally, the reduced hardness across the Nb interlayer of the Ti/Nb/SS weld versus the Nb/SS weld appears to result from annealing effects provided by the Ti/Nb weld thermal cycle.

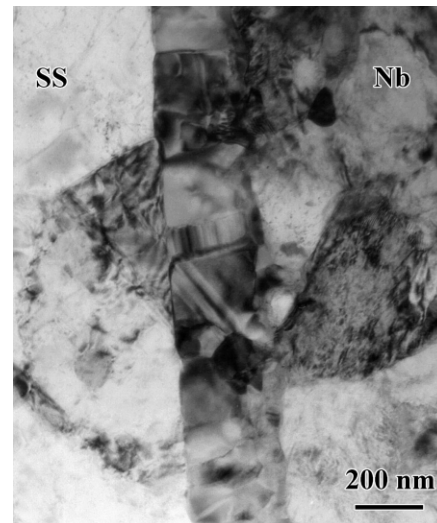


Figure 3. TEM micrograph of 316L SS/Nb interface.

### 3.4 Tensile Testing

Room temperature uniaxial tensile test results ranged from 338 to 527 MPa. Failure occurred in both the Ti base metal and through the interlayer metal. Specimens failing through the interlayer exhibited considerable reduction in area in the Ti base metal away from the interface. Since there was no noticeable reduction in area in the SS, it appears to have constrained the Nb interlayer thus transferring strain/stress to the Ti, hence, the joint's tensile strength was appreciably higher than would be expected from a tensile test of a monolithic Nb tube.

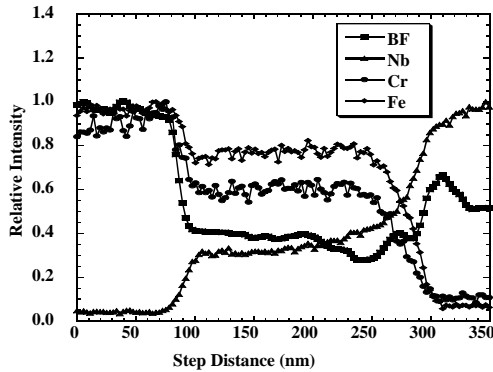


Figure 4. STEM line scans across the interaction layer. BF represents bright field image.

### 3.5 Fracture Analysis

An SEM fractograph of a Ti/Nb/SS weld tensile test specimen that failed through the interlayer region is shown in Figure 6. Microscopically, the fracture surface exhibited two fracture surface topographies. At some locations, a relatively flat smooth surface was exhibited. Tear ridges separated regions of flat, nearly featureless fracture and regions of microvoids. The microvoids had nucleated in the soft Nb interlayer.

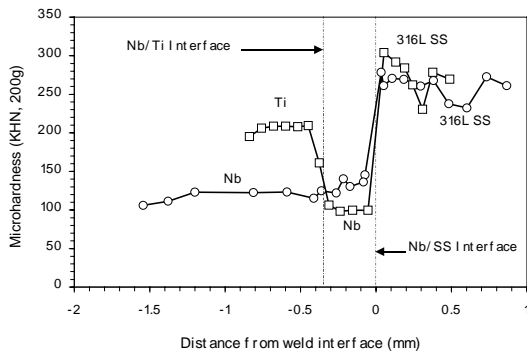


Figure 5. Microhardness traverses across weld joints.

## 4. CONCLUSIONS

From the results of light and analytical electron microscopy, and mechanical property evaluations, the following conclusions can be drawn:

1. Using conventional IFR welding techniques, 316L SS was successfully joined to Nb and to commercially pure Ti using an interlayer of Nb;
2. The inherent solid-state nature and rapid thermal cycle afforded by IFR welding restricted base-metal interdiffusion, however, STEM results revealed a thin (200-nm) intermetallic phase of Nb(Fe,Cr)<sub>2</sub> between the 316L SS base metal and Nb interlayer;
3. STEM results also revealed a uniform distribution of Fe, Cr and Nb across the NbFe<sub>2</sub> Laves-type interaction layer;
4. The favorable results permit use of Ti/316L SS joints and Nb/316L SS joints in a superconducting cavity and cryomodule chosen as a candidate for the Department of Energy's accelerator production of tritium program.

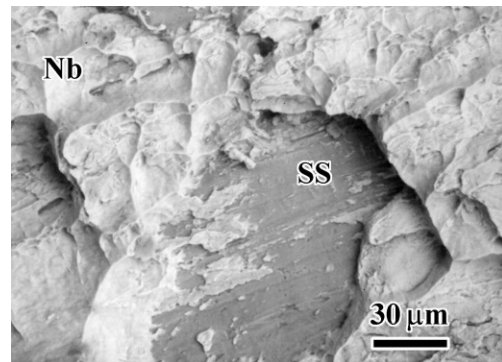


Figure 6. Fractograph of Ti/Nb/SS IFR weld. Fracture was through the Nb interlayer region.

## 5. ACKNOWLEDGEMENTS

This research was funded under DOE contract no. W-7406-ENG-36. The authors wish to thank Ms. Ann Kelly and Ms. Pallas Papin for their experimental assistance.

## 6. REFERENCES

1. Akizuki, S. *et al*, "Welding between titanium and mild steel", *Titanium and Zirconium* 10 (9) 31-36 (1962)
2. Akizuki, S. *et al*, "Welding between titanium and steel", *Titanium and Zirconium* 10 (9) 8-14 (1962)
3. Futamata, M. and Fuji, A., "Friction welding of titanium and SUS 304L austenitic stainless steel", *Welding Int'l*, 4 (10) 768-774 (1990)
4. Fuji, A. *et al*, "Improving tensile strength and bend ductility of titanium/AISI 304L stainless steel friction welds", *MS&T* 3 (8) 219-235 (1992)
5. Fuji, A., *et al*, "Improved mechanical properties in dissimilar Ti-AISI 304L joints", *J.Mat.Sc.* 31 819-827 (1996)
6. Sassani, F. and Neelam, J.R., "Friction welding of incompatible materials", *WJ*, 11 264s-270s (1988)
7. Kou, M., "Dissimilar friction welding of titanium alloys to Alloy 718", PhD Dissertation, The Ohio State University, (1993)